

# Turning G Proteins On and Off Using Peptide Ligands

William W. Ja<sup>†,‡,¶</sup>, Ofer Wiser<sup>\*,‡,¶,¶</sup>, Ryan J. Austin<sup>†</sup>, Lily Y. Jan<sup>‡</sup>, and Richard W. Roberts<sup>§,¶</sup>

<sup>†</sup>Division of Biology, California Institute of Technology, Pasadena, California 91125, <sup>‡</sup>Howard Hughes Medical Institute, Departments of Physiology and Biochemistry, University of California, San Francisco, 1550 Fourth Street, San Francisco, California 94143 and

<sup>§</sup>Department of Chemistry and Mork Family Department of Chemical Engineering, University of Southern California, Los Angeles, California 90089, <sup>¶</sup>Current address: Goldyne Savad Institute of Gene Therapy, Hadassah University Hospital, P.O. Box 12000, Jerusalem 91120, Israel, <sup>||</sup>These authors contributed equally to this work

**ABSTRACT** Intracellular G $\alpha$  subunits represent potential therapeutic targets for a number of diseases. Here we describe three classes of new molecules that modulate G protein signaling by direct targeting of G $\alpha$ . Using messenger RNA display, we have identified unique peptide sequences that bind G $\alpha_{i1}$ . Functionally, individual peptides were found that either enhance or repress basal levels of G protein-activated inwardly rectifying potassium (GIRK) channel signaling, a downstream effector of G protein activation, indicating that the peptides directly turn G proteins on or off *in vivo*. A third functional class acts as a signaling attenuator; basal GIRK channel activity is unaffected but responses to repeated G protein activation are reduced. These data demonstrate that G protein-directed ligands can achieve physiological effects similar to those resulting from classical receptor targeting and may serve as leads for developing new classes of therapeutics.

Heterotrimeric guanine nucleotide-binding proteins (G proteins), composed of  $\alpha$ ,  $\beta$ , and  $\gamma$  subunits, play a critical role in communicating extracellular signals to intracellular signal transduction pathways through membrane-spanning G protein-coupled receptors (GPCRs) (1, 2). Activation of GPCRs by extracellular agonists triggers the exchange of GDP with GTP in the G $\alpha$  subunit and dissociation of G $\beta\gamma$  heterodimers from G $\alpha$ -GTP, which both regulate multiple effectors. G $\beta\gamma$  subunits, for example, can directly regulate adenylyl cyclase, phospholipase C $\beta$  isozymes, and G protein-activated inwardly rectifying potassium (GIRK) channels (3). GTP hydrolysis by the inherent G $\alpha$  GTPase activity, a reaction catalyzed by various GTPase-activating proteins (GAPs), returns G $\alpha$  to the GDP-bound state and results in reassociation with G $\beta\gamma$  and termination of signaling.

Intracellular G proteins have potential as drug targets for a number of diseases (4–7). The large number of possible combinations of  $\alpha$ ,  $\beta$ , and  $\gamma$  subunits suggests that direct G protein ligands could affect individual effector pathways and/or modify signaling kinetics with great specificity (5, 8, 9). The G protein regulatory (GPR) or GoLoco motif, for example, is a peptide guanine nucleotide dissociation inhibitor (GDI) that is implicated in receptor-independent signaling (10, 11). Other recent advances include the identification of ligands for G $\beta\gamma$  that affect downstream signaling pathways using peptide (12) or small molecule (13) libraries.

*In vitro* peptide selection methods have been widely successful in isolating ligands for biological targets (14, 15). Various proteins in the G protein signaling pathway have been targeted by selection libraries, including receptors and G $\alpha$  and G $\beta\gamma$  subunits (8). Messenger RNA (mRNA) display is a selection technique where each peptide in a library is covalently coupled with its encoding mRNA (16, 17). Previously, we used mRNA display selection to identify a peptide (R6A) and its core motif (R6A-1) that bind with high affinity and specificity to the GDP-state of G $\alpha$  subunits (18, 19). R6A and R6A-1 act as GDIs and compete with G $\beta\gamma$  for binding to G $\alpha_{i1}$  (18, 19). We hypothesized that the 9-residue R6A-1 sequence could be used as a scaffold for developing new peptide ligands with different activities and/or specificities for G $\alpha$  subunits. Here we design an mRNA display library based on the R6A-1 core motif and use *in vitro* selection to identify unique peptides that differentially modulate G protein signaling.

A DNA template was constructed to encode the R6A-1 peptide (DQLYWWEYL) flanked by random hexamers on each end (see Methods). Nucleotide incorporation was controlled such that each wild-type residue in the core motif was ~40–50% conserved (20). mRNA display selection was performed on N-terminally biotinylated G $\alpha_{i1}$  (Nb-G $\alpha_{i1}$ ) due to the previous finding that R6A-derived peptides bind preferentially to Nb-G $\alpha_{i1}$  over the C-terminally biotinylated Cb-G $\alpha_{i1}$  (18). Aluminum fluoride (AlF) was

\*Corresponding author,  
richrob@usc.edu.

Received for review September 8, 2006  
and accepted September 18, 2006.

Published online October 20, 2006  
10.1021/cb600345k CCC: \$33.50

© 2006 by American Chemical Society

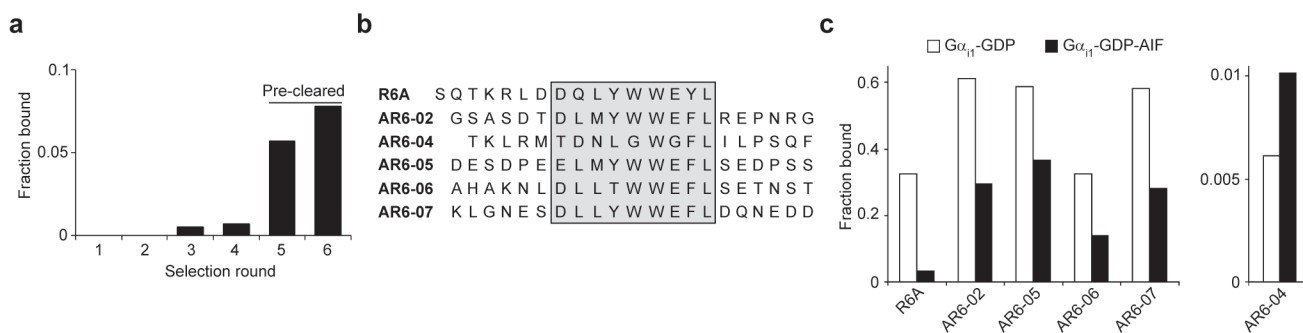


**Figure 1.** *In vitro* selection targeting  $G\alpha_{11}$ -GDP-AIF. **a)** Fraction of  $^{35}\text{S}$ -Met-labeled mRNA display pools from each round of selection bound to immobilized  $G\alpha_{11}$ -GDP-AIF and recovered by elution with SDS. The inputs for the fifth and sixth rounds were precleared against  $G\alpha_{11}$ -GDP prior to selection. **b)** Sequences of peptides used in *in vitro* studies. The region corresponding to the R6A-1 core motif is boxed (gray). The C-terminal constant region is not shown. **c)** Binding of individual, RNase-treated,  $^{35}\text{S}$ -Met-labeled mRNA display fusions to  $G\alpha_{11}$ -GDP or  $G\alpha_{11}$ -GDP-AIF. Except for AR6-04, all tested peptides have a preference for binding to  $G\alpha_{11}$ -GDP.

supplemented into the selection buffer to attempt to select for peptides specific for the GDP-AIF state of  $G\alpha_{11}$ , a transition state mimic of GTP hydrolysis (21, 22). AIF (either as AIF<sub>3</sub> or AIF<sub>4</sub><sup>-</sup>) has been shown to activate  $G\alpha$  subunits, preventing association with  $G\beta\gamma$  heterodimers, and GAPs have been shown to bind exclusively to this transition state mimic. Six rounds of selection were performed, and significant binding was observed by the third round (Figure 1, panel a). On the basis of the starting library complexity of  $\sim 2 \times 10^{13}$  and a maximum enrichment of 10,000-fold per round, we estimate that the third-round input pool contained >100,000 unique,  $G\alpha_{11}$ -binding peptide sequences. To enrich for peptides specific for the AIF-bound state of  $G\alpha_{11}$ , the fifth- and sixth-round pools were precleared against  $G\alpha_{11}$ -GDP prior to selection against  $G\alpha_{11}$ -GDP-AIF.

DNA sequencing of clones from the sixth-round pool showed that the core 9-mer was primarily conserved, except for a preference for leucine instead of glutamine in the second position (Figure 1, panel b and Supplementary Table 1). The random hexamer regions showed no obvious sequence conservation, although the residues directly flanking the core motif favored several amino acids, including leucine,

aspartate, and glutamate. *In vitro* binding assays with individual clones revealed that the peptides bind  $\sim 1$ –40% to immobilized  $G\alpha_{11}$ -GDP-AIF (Figure 1, panel c). The wide range of binding may suggest that the selection was not complete or that specificity to the AIF-bound state of  $G\alpha_{11}$  produces a trade-off in overall binding.

Binding assays of individual peptides to  $G\alpha_{11}$ -GDP in the presence or absence of AIF

show that most peptides favor the GDP-bound state (Figure 1, panel c). Hence, the selection identified peptides with a loss of specificity compared with the original R6A sequence. Only one peptide, AR6-04, exhibited better binding in the presence of AIF, but this peptide appears to have an affinity for  $G\alpha_{11}$  significantly lower than that of other peptides. Because the selected peptides bind both states, preclearing the fifth- and

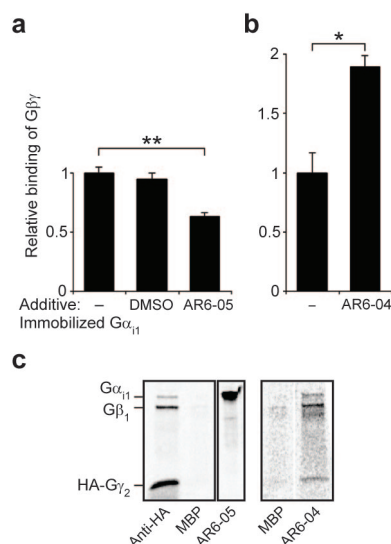


**Figure 2.** AR6-04 and AR6-05  $G\alpha_{11}$ -binding peptides differentially affect  $G\beta\gamma$  association. **a, b)** Binding of  $^{35}\text{S}$ -Met-labeled  $G\beta_1\gamma_2$  to immobilized  $G\alpha_{11}$  in the presence or absence of AR6-05 (20  $\mu\text{M}$ ) or AR6-04 (33  $\mu\text{M}$ ). AR6-05 competes with  $G\beta\gamma$  for association to  $G\alpha_{11}$  ( $n = 4$ ,  $p = 0.0050$ ), whereas AR6-04 increases  $G\beta\gamma$  binding ( $n = 3$ ,  $p = 0.041$ ). DMSO ( $\sim 1\%$ , v/v) had no effect on  $G\beta\gamma$  binding ( $n = 3$ ,  $p = 0.50$ ). **c)** Binding of  $^{35}\text{S}$ -Met-labeled  $G\alpha_{11}\beta_1\gamma_2$  to immobilized peptides. Anti-hemagglutinin (HA) antibody immunoprecipitates the HA-tagged  $G\gamma_2$  subunit and confirms the presence of reconstituted heterotrimers. Immobilized maltose-binding protein (MBP) fails to pull down G proteins, while binding of  $G\alpha_{11}$  to immobilized AR6-05-MBP completely precludes  $G\beta_1\gamma_2$  association. AR6-04-MBP, however, pulls down the intact heterotrimer. The control MBP lane is shown again at the same contrast as the AR6-04 lane for comparison.

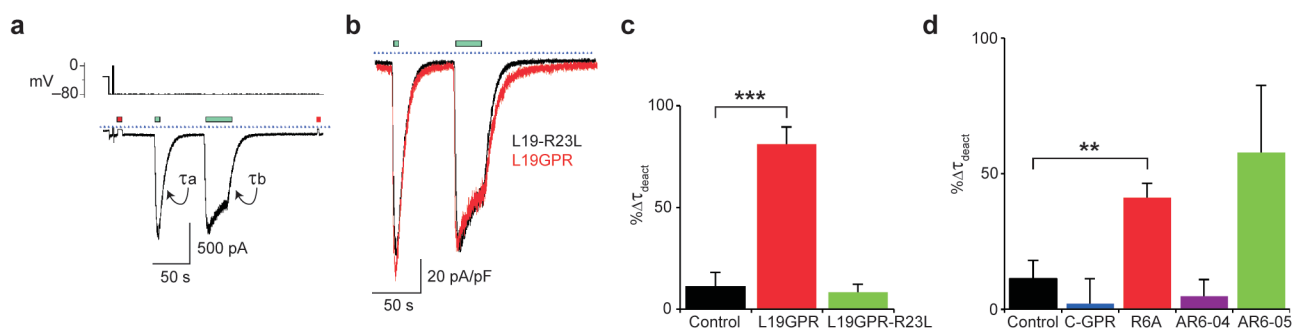


**Figure 3.** Effect of intracellular application of peptides on GIRK deactivation kinetics. **a)** HEK293 cells stably expressing GIRK1 and 2 and the dopamine receptor  $D_{2s}$  were recorded by whole-cell patch-clamp (see Methods). Zero- $K^+$  buffer (red bar) was perfused for 4 s to determine GIRK basal activity. Application of dopamine for 4 and 30 s (green bars) activated GIRK currents. Dopamine washout was followed by GIRK channel deactivation.  $\tau_a$  and  $\tau_b$  are the GIRK deactivation time constants following the short and long dopamine applications, respectively. The dotted line represents 0 pA. **b)** Superposition of representative current traces of cells recorded in the presence of 2  $\mu$ M of the control peptide L19GPR-R23L (black) or the L19GPR peptide (red). L19GPR-R23L is a negative control peptide that contains a mutation to a critical arginine residue (26). Current traces were normalized to cell membrane capacitance and current amplitude in Zero- $K^+$  buffer was subtracted from current traces in High- $K^+$  buffer. **c)** L19GPR (2  $\mu$ M) increases  $\tau_b$  after prolonged dopamine application ( $n = 7$ ,  $p = 3.9 \times 10^{-5}$ ), whereas the control L19GPR-R23L peptide (2  $\mu$ M) has no effect ( $n = 2$ ,  $p = 0.71$ ).  $\% \Delta \tau_{\text{deact}}$  is the percentage change of  $\tau_b$  from  $\tau_a$ . **d)** R6A (100  $\mu$ M) moderately increases  $\tau_b$  ( $n = 4$ ,  $p = 0.0065$ ), whereas AR6-04 (40  $\mu$ M,  $n = 5$ ,  $p = 0.49$ ) and the control C-GPR peptide (100  $\mu$ M,  $n = 5$ ,  $p = 0.44$ ) have no effect. AR6-05 (40  $\mu$ M) appears to increase  $\tau_b$  ( $n = 5$ ,  $p = 0.13$ ), but there is significantly increased error in the kinetics measurements likely due to the effect that AR6-05 has on basal GIRK activity. In panels c and d, the control contains  $<0.5\%$  (v/v) DMSO.

sixth-round pools on  $G\alpha_{i1}$ -GDP may have removed the highest affinity peptides while only marginally enriching for specificity to  $G\alpha_{i1}$ -GDP-AIF.

AR6-04 and AR6-05 exhibited the highest AIF/GDP-state binding ratios for  $G\alpha_{i1}$  and were synthesized for further characterization. Their affinities to immobilized  $G\alpha_{i1}$ -GDP were determined by surface plasmon resonance (SPR). Corresponding with the lower binding seen in the *in vitro* assays, the  $K_D$  of AR6-04 for  $G\alpha_{i1}$ -GDP appears to be  $>10 \mu$ M. Conversely, AR6-05, with an apparent  $K_D$  of  $\sim 10$  nM, is the highest affinity  $G\alpha$ -directed peptide that we have tested, binding  $>6$ -fold better to  $G\alpha_{i1}$ -GDP than our previously described R6A peptide and  $>20$ -fold better than the R6A-1 core motif (18). Whereas R6A and R6A-1 show clear 1:1 bimolecular binding kinetics, AR6-05 binding data were well fit only with a more complex kinetics model (Supplementary Figure 1).

R6A and R6A-1 were previously shown to compete with  $G\beta\gamma$  heterodimers for binding

to  $G\alpha_{i1}$  *in vitro* (18, 19). Binding of radiolabeled  $G\beta_1\gamma_2$  to immobilized  $G\alpha_{i1}$  in the presence or absence of peptides was performed to determine the peptide effects on  $G\beta\gamma$  association. AR6-05 competes with  $G\beta\gamma$  for binding to  $G\alpha_{i1}$  (Figure 2, panel a). Like the R6A peptide, binding of  $G\alpha_{i1}$  to immobilized AR6-05 precludes  $G\beta\gamma$  association (Figure 2, panel c).

Surprisingly, AR6-04 appears to enhance  $G\beta_1\gamma_2$  binding to  $G\alpha_{i1}$ . Several *in vitro* assays were performed that support this observation: (i) labeled  $G\beta\gamma$  shows higher binding to immobilized  $G\alpha_{i1}$  in the presence of free AR6-04 peptide (Figure 2, panel b), (ii) labeled AR6-04 peptide shows 66% higher binding to immobilized  $G\alpha_{i1}$  in the presence of  $G\beta_1\gamma_2$ , and (iii) experiments with labeled  $G\alpha_{i1}\beta_1\gamma_2$  show that immobilized AR6-04 is able to pull down all three subunits (Figure 2, panel c).

To test the activity of the peptides in a cellular context, we used a HEK293 cell line expressing GIRK1 and 2 and the dopamine  $D_{2s}$  GPCR. Previous cell culture studies have

shown that, similar to the G protein specificity observed *in vivo*, only  $G_{i/o}$ -coupled receptors activate GIRK channels (23, 24). In these cells, GIRK channels are the dominant downstream effectors of released  $G\beta\gamma$  subunits. The GPR consensus peptide (10) was previously shown to attenuate signaling events after an initial agonist application, without affecting basal GIRK activity (25). The authors hypothesized that the GPR peptide is able to interact with  $G\alpha$  subunits only after an initial activation, which frees  $G\alpha$  for peptide binding. We confirmed these results with the L19GPR peptide, which differs from the GPR consensus at a redundant residue (10, 18, 26). In the absence of peptide, the kinetics of channel deactivation ( $\tau$ , deactivation time constant) are similar after short ( $\tau_a$ ) followed by long ( $\tau_b$ ) dopamine applications ( $10.6 \pm 1.9$  s,  $n = 10$  and  $13.7 \pm 3.4$  s,  $n = 7$ , respectively,  $p = 0.68$ ; Figure 3, panel a). In contrast, L19GPR increased  $\tau_b$  significantly compared with controls (Figure 3, panels b and c). GIRK basal activity returned to its initial values

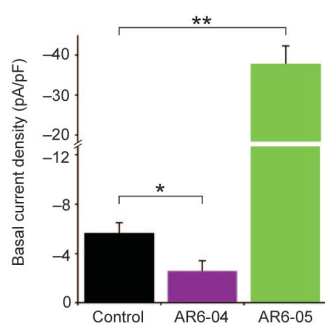


**Figure 4.** Intracellular application of 40  $\mu\text{M}$  AR6-05 or AR6-04 increases ( $n = 4$ ,  $p = 0.0046$ ) or decreases ( $n = 5$ ,  $p = 0.027$ ) basal GIRK currents, respectively. Current densities are determined by normalization with the individual cell capacitance. The control contains <0.5% (v/v) DMSO.

after  $\sim 2$  min from the dopamine washout, indicating that the L19GPR peptide effect is transient, since a persistent effect should have resulted in higher basal activity.

R6A exhibited effects similar to those of the L19GPR peptide. R6A increased  $\tau_b$  moderately, whereas the negative control peptide C-GPR had no effect (Figure 3, panel d). R6A had minimal effect on the basal GIRK channel activity ( $n = 7$ ,  $p = 0.18$ ), which suggests that, like the GPR peptide, R6A is unable to dissociate  $G\alpha\beta\gamma$  heterotrimers *in vivo*. In contrast to R6A, intracellular application of AR6-05 increased basal activity dramatically, suggesting that AR6-05 actively dissociates  $G\beta\gamma$  from  $G\alpha$  *in vivo* (Figure 4).

AR6-04 had no effect on the deactivation kinetics (Figure 3, panel d) but instead directly reduced basal GIRK activity (Figure 4). This coincides with the *in vitro* binding data, where AR6-04 stabilizes a heterotrimer complex and presumably reduces the active  $G\beta\gamma$  available for GIRK channel activation. It is not clear how AR6-04 stabilizes the heterotrimer despite being selected against the  $G\alpha$  subunit alone. The peptide sequence differs greatly from the original R6A-1 core motif. The flanking regions of AR6-04, however, share modest sequence similarity to

the short  $G\beta\gamma$ -binding motifs previously identified (12), suggesting that other molecules that shut down G protein signaling may be constructed by fusing known  $G\alpha$ - and  $G\beta\gamma$ -specific ligands.

The R6A-1 based peptide library should be useful for the selection of peptides that are specific for various G protein subclasses or nucleotide-bound states. Distinct functions, such as specificity for  $G\alpha_{i1}$  over other  $G\alpha$  subunits, may not yet be identified from the large number of unique  $G\alpha_{i1}$ -binding peptides recovered in our selection. While it is clear that AR6-04 and AR6-05 affect GIRK channel activity, an effector of  $G\beta\gamma$ , the peptide effects on  $G\alpha$ -regulated pathways and  $G\alpha$  nucleotide-bound states have yet to be determined. For example, because GAPs have been shown to catalyze GTP hydrolysis by stabilizing a transition state (21, 22), selected peptides that bind  $G\alpha_{i1}$ -GDP-AIF may act as small-molecule GAPs. Although further technological advances are necessary for the facile conversion of peptides to therapeutics, determining the mechanism of action of the AR6-04 and AR6-05 peptides will facilitate the rational design of more potent modulators of G protein signaling for use as biological tools and potential drug leads.

## METHODS

**Materials.** Human complementary DNA (cDNA) clones for G proteins were obtained from the University of Missouri-Rolla cDNA Resource Center ([www.cdna.org](http://www.cdna.org)) in the pcDNA3.1+ vector (Invitrogen). The  $G\gamma_2$  cDNA vector encoded an N-terminal HA tag. Anti-HA monoclonal antibody (clone HA-7) was obtained from Sigma. Expression of  $^{35}\text{S}$ -Met labeled G proteins by *in vitro* translation was performed as described previously (19).

**mRNA Display Selection.** The doped R6A-1 library was constructed by polymerase chain reaction amplification of oligo 115.1 [5'-AGC AGA GAC ACT AGT GTA ACC GCC (SNN)<sub>6</sub> (S13) (641) (542) (521) (521) (641) (S13) (543) (642) (SNN)<sub>6</sub> CAT TGT AAT TGT AAA TAG TAA TTG TCC C; 1 = 7:1:1:1, 2 = 1:7:1:1, 3 = 1:1:7:1, 4 = 1:1:1:7, A:C:G:T; 5 = 9:1, 6 = 1:9, C:G; N = A, C, G, OR T; S = C or G (ratios have been adjusted for synthesis incorporation rates)] with primers 47T7FP (5'-GGA TTC TAA TAC GAC TCA CTA TAG GGA CAA TTA CTA TTT ACA ATT AC) and 22.9 (5'-AGC AGA CAG ACT AGT GTA ACC G) to produce double-stranded DNA encoding

M-X<sub>6</sub>-DQLYWWEYL-X<sub>6</sub>-GGYTSLSA, with the core 9-residues conserved  $\sim 40$ –50%. Sequencing of randomly chosen clones from the initial pool revealed a distribution of wild-type residues in the core motif that agreed with theoretical calculations (data not shown). *In vitro* transcription, ligation of the mRNA to the puromycin linker, and purification of the RNA-F30P template were performed as described previously, except that the splint oligo 23.8 (5'-TTT TTT TTT TTN AGC AGA CAG AC) was used for the ligation reaction (18). RNA-peptide fusions were prepared, purified on oligo-dT cellulose, reverse-transcribed with oligo 22.9, and selected against immobilized Nb- $G\alpha_{i1}$  as described previously using a modified selection buffer [25 mM 4-(2-hydroxyethyl)-1-piperazineethanesulfonic acid (HEPES)-KOH at pH 7.5, 150 mM NaCl, 0.05% (v/v) Tween 20, 1 mM  $\beta$ -mercaptoethanol, 10  $\mu\text{M}$  GDP, 20  $\mu\text{M}$  EDTA, 5 mM  $\text{MgCl}_2$ , 10 mM NaF, 25  $\mu\text{M}$   $\text{AlCl}_3$ , 0.05% (w/v) bovine serum albumin, and 1 mg  $\text{mL}^{-1}$  yeast transfer RNA] (18).

**RNA-Peptide Fusion Binding Assay.** Purified RNase-treated mRNA display peptide fusions of individual clones were assayed for binding as described previously (27). Briefly, aliquots of  $^{35}\text{S}$ -labeled fusions were added to  $\sim 15$   $\mu\text{L}$  of Nb- $G\alpha_{i1}$  ( $\sim 15$   $\mu\text{g}$  protein) on streptavidin agarose (immobilized NeutrAvidin on agarose, Pierce) in 1 mL of selection buffer. After binding for 1 h, the matrices were washed with  $3 \times 0.6$  mL of selection buffer in a 0.45  $\mu\text{m}$  cellulose acetate spin filter (CoStar Spin-X, Corning). Input  $^{35}\text{S}$  counts for binding assays were determined by scintillation counting of the washes and the matrix. Bound  $^{35}\text{S}$  counts were divided by the input counts to calculate the fraction bound. Binding of RNase-treated peptide fusions to the immobilization matrix alone was  $<0.001$ . Assays for binding to  $G\alpha_{i1}$ -GDP were performed in selection buffer without AIF.

**In Vitro Peptide Studies.** Peptides were synthesized with the first three residues of the C-terminal constant tag (GGY) and purified by Bio-Synthesis, Inc. Three additional C-terminal lysines were added to the AR6-04 peptide to enhance solubility. SPR affinity measurements were made on immobilized Nb- $G\alpha_{i1}$  as described previously (18). Peptide effects on  $G\beta\gamma$  association with immobilized Nb- $G\alpha_{i1}$  were assayed by mixing an aliquot of  $^{35}\text{S}$ -labeled  $G\beta_1\gamma_2$  with  $\sim 15$   $\mu\text{L}$  of immobilized Nb- $G\alpha_{i1}$  in 1 mL of selection buffer without AIF. After rotating at 4  $^\circ\text{C}$  for 1 h, samples were washed with  $3 \times 0.6$  mL of the binding buffer in a spin filter, as described above. Binding was determined by scintillation counting and scaled to the amount of  $G\beta\gamma$  pulled down in the absence of peptide. Data are background subtracted from binding to matrix without immobilized  $G\alpha_{i1}$  ( $\sim 10\%$  of overall binding). AIF reduced  $G\beta_1\gamma_2$  pull down on Nb- $G\alpha_{i1}$  to  $\sim 50\%$ .

**$G\alpha\beta\gamma$  Heterotrimer Immunoprecipitation.** AR6-04 and AR6-05 were expressed as MBP fusion proteins and immobilized by random amine coupling on CNBr-Sepharose 4B (GE Healthcare) as described previously (19).  $^{35}\text{S}$ -Labeled  $G\alpha\beta\gamma$  heterotrimer was immunoprecipitated with anti-HA monoclonal antibody and protein G-sepharose or pulled down on immobilized MBP as described

previously (19). Recovered proteins were separated by SDS-PAGE. Gels were imaged by autoradiography (Storm PhosphorImager, GE Healthcare).

**Electrophysiology.** We used HEK293 cell lines stably expressing GIRK1, GIRK2a, and the  $G_{i/o}$ -coupled dopamine ( $D_{2c}$ ) receptor (23). The pipet solution contained 107 mM KCl, 1.2 mM  $MgCl_2$ , 1 mM  $CaCl_2$ , 10 mM EGTA, 5 mM HEPES at pH 7.4, 2 mM MgATP, and 0.3 mM  $Na_2GTP$ . Peptides were added to the pipet solution immediately prior to recording. The final DMSO concentration was 0.5% (v/v) or less. The bath solution contained 2.6 mM  $CaCl_2$ , 1.2 mM  $MgCl_2$ , 5 mM HEPES at pH 7.4, and either 140 mM KCl (High- $K^+$ ) or 140 mM NaCl (Zero- $K^+$ ). Membrane currents were recorded in a whole-cell patch-clamp mode with an Axopatch 200B amplifier (Axon Instruments) and a patch pipet resistance of 2.5–4.5 M $\Omega$ . Data were filtered at 1 kHz and digitized at 5 kHz. Cell capacitance was 12–18 pF, and series resistance (5–20 M $\Omega$ ) was at least 75% compensated on-line. Current recording was acquired after equilibration for ~5 min in gap-free mode at –80 mV. Dopamine (2  $\mu$ M, Sigma) was applied in bath solution via an  $N_2$ -pressurized perfusion system (ALA Scientific Instruments).

**Data Analysis.** Data acquisition and analysis was done by a Digidata 1200A interface (Axon Instruments) and pClamp 8.2 and Microcal Origin 6.0 software. The deactivation time constants ( $\tau$ ) were determined in pClamp (standard exponential). Currents were averaged over 17 ms to reduce 60 Hz background noise. All data are presented as mean  $\pm$  SEM. Statistical significance was determined by non-paired, two-tailed Student's *t* tests. Significance in figures: \*,  $p < 0.05$ ; \*\*,  $p < 0.01$ ; \*\*\*,  $p < 0.0001$ .

**Acknowledgment:** We thank D. S. Waugh (National Cancer Institute at Frederick) for providing the original pDW363 vector and P. J. Bjorkman for the use of the Biacore 2000 instrument. This work was supported by funding from the National Institutes of Health (GM60416) and the Beckman Foundation (R.W.R.), the Howard Hughes Medical Institute and National Institute of Mental Health (MH63981) (L.Y.J., in the Silvio Conte Center of Neuroscience at the University of California-San Francisco), the European Molecular Biology Organization (O.W.), and a Department of Defense National Defense Science and Engineering Graduate Fellowship (W.W.J.).

**Supporting Information Available:** This material is available free of charge via the Internet.

## REFERENCES

- Gilman, A. G. (1987) G proteins: transducers of receptor-generated signals, *Annu. Rev. Biochem.* 56, 615–649.
- Neves, S. R., Ram, P. T., and Iyengar, R. (2002) G protein pathways, *Science* 296, 1636–1639.
- Clapham, D. E., and Neer, E. J. (1997) G protein  $\beta\gamma$  subunits, *Annu. Rev. Pharmacol. Toxicol.* 37, 167–203.
- Nürnberg, B., Tögel, W., Krause, G., Storm, R., Breitweg-Lehmann, E., and Schunack, W. (1999) Non-peptide G-protein activators as promising tools in cell biology and potential drug leads, *Eur. J. Med. Chem.* 34, 5–30.
- Höller, C., Freissmuth, M., and Nanoff, C. (1999) G proteins as drug targets, *Cell. Mol. Life Sci.* 55, 257–270.
- Freissmuth, M., Waldhoer, M., Bofill-Cardona, E., and Nanoff, C. (1999) G protein antagonists, *Trends Pharmacol. Sci.* 20, 237–245.
- Spiegel, A. M., and Weinstein, L. S. (2004) Inherited diseases involving G proteins and G protein-coupled receptors, *Annu. Rev. Med.* 55, 27–39.
- Ja, W. W., and Roberts, R. W. (2005) G-protein-directed ligand discovery with peptide combinatorial libraries, *Trends Biochem. Sci.* 30, 318–324.
- Chahdi, A., Daeflter, L., Gies, J. P., and Landry, Y. (1998) Drugs interacting with G protein  $\alpha$  subunits: selectivity and perspectives, *Fundam. Clin. Pharmacol.* 12, 121–132.
- Peterson, Y. K., Bernard, M. L., Ma, H., Hazard, S., III, Graber, S. G., and Lanier, S. M. (2000) Stabilization of the GDP-bound conformation of  $G_{i\alpha}$  by a peptide derived from the G-protein regulatory motif of AGS3, *J. Biol. Chem.* 275, 33193–33196.
- Willard, F. S., Kimple, R. J., and Siderovski, D. P. (2004) Return of the GDI: the GoLoco motif in cell division, *Annu. Rev. Biochem.* 73, 925–951.
- Scott, J. K., Huang, S. F., Gangadhar, B. P., Samoriski, G. M., Clapp, P., Gross, R. A., Taussig, R., and Smrcka, A. V. (2001) Evidence that a protein-protein interaction 'hot spot' on heterotrimeric G protein beta gamma subunits is used for recognition of a subclass of effectors, *EMBO J.* 20, 767–776.
- Bonacci, T. M., Mathews, J. L., Yuan, C., Lehmann, D. M., Malik, S., Wu, D., Font, J. L., Bidlack, J. M., and Smrcka, A. V. (2006) Differential targeting of  $G\beta\gamma$ -subunit signaling with small molecules, *Science* 312, 443–446.
- Dower, W. J., and Mattheakis, L. C. (2002) *In vitro* selection as a powerful tool for the applied evolution of proteins and peptides, *Curr. Opin. Chem. Biol.* 6, 390–398.
- Lin, H., and Comish, V. W. (2002) Screening and selection methods for large-scale analysis of protein function, *Angew. Chem., Int. Ed.* 41, 4402–4425.
- Roberts, R. W., and Szostak, J. W. (1997) RNA-peptide fusions for the *in vitro* selection of peptides and proteins, *Proc. Natl. Acad. Sci. U.S.A.* 94, 12297–12302.
- Takahashi, T. T., Austin, R. J., and Roberts, R. W. (2003) mRNA display: ligand discovery, interaction analysis and beyond, *Trends Biochem. Sci.* 28, 159–165.
- Ja, W. W., and Roberts, R. W. (2004) *In vitro* selection of state-specific peptide modulators of G protein signaling using mRNA display, *Biochemistry* 43, 9265–9275.
- Ja, W. W., Adhikari, A., Austin, R. J., Sprang, S. R., and Roberts, R. W. (2005) A peptide core motif for binding to heterotrimeric G protein  $\alpha$  subunits, *J. Biol. Chem.* 280, 32057–32060.
- LaBean, T. H., and Kauffman, S. A. (1993) Design of synthetic gene libraries encoding random sequence proteins with desired ensemble characteristics, *Protein Sci.* 2, 1249–1254.
- Berman, D. M., Kozasa, T., and Gilman, A. G. (1996) The GTPase-activating protein RGS4 stabilizes the transition state for nucleotide hydrolysis, *J. Biol. Chem.* 271, 27209–27212.
- Tesmer, J. J. G., Berman, D. M., Gilman, A. G., and Sprang, S. R. (1997) Structure of RGS4 bound to  $AlF_4^+$ -activated  $G_{i\alpha 1}$ : stabilization of the transition state for GTP hydrolysis, *Cell* 89, 251–261.
- Leaney, J. L., Milligan, G., and Tinker, A. (2000) The G protein  $\alpha$  subunit has a key role in determining the specificity of coupling to, but not the activation of, G protein-gated inwardly rectifying  $K^+$  channels, *J. Biol. Chem.* 275, 921–929.
- Benians, A., Leaney, J. L., and Tinker, A. (2003) Agonist unbinding from receptor dictates the nature of deactivation kinetics of G protein-gated  $K^+$  channels, *Proc. Natl. Acad. Sci. U.S.A.* 100, 6239–6244.
- Webb, C. K., McCudden, C. R., Willard, F. S., Kimple, R. J., Siderovski, D. P., and Oxford, G. S. (2005) D2 dopamine receptor activation of potassium channels is selectively decoupled by  $G\alpha_i$ -specific GoLoco motif peptides, *J. Neurochem.* 92, 1408–1418.
- Peterson, Y. K., Hazard, S., III, Graber, S. G., and Lanier, S. M. (2002) Identification of structural features in the G-protein regulatory motif required for regulation of heterotrimeric G-proteins, *J. Biol. Chem.* 277, 6767–6770.
- Ja, W. W., Olsen, B. N., and Roberts, R. W. (2005) Epitope mapping using mRNA display and a unidirectional nested deletion library, *Protein Eng. Des. Sel.* 18, 309–319.